2019 American Control Conference (ACC)
Philadelphia, PA, USA, July 10-12, 2019

# Closed Form Time Response of an Infinite Tree of Mechanical Components Described by an Irrational Transfer Function

A.-J. Guel-Cortez,[1] Mihir Sen[2] and Bill Goodwine[2]

***Abstract*— In this work we determine the time-domain dynamics of a complex mechanical network of integer-order components, e.g., springs and dampers, with an overall transfer function described by implicitly defined operators. This type of transfer functions can be used to describe very large scale dynamics of robot formations, multi-agent systems or viscoelastic phenomena. Such large-scale integrated systems are becoming increasingly important in modern engineering systems, and an accurate model of their dynamics is very important to achieve their control. We give a time domain representation for the dynamics of the system by using a complex variable analysis to find its impulse response. Furthermore, we validate how our infinite order model can be used to describe dynamics of finite order networks, which can be useful as a model reduction method.**

## I. INTRODUCTION

Important modern engineering problems deal with systems or phenomena that consists of many interacting components with coupled dynamics which are often impractical or intractable to model. Examples of such systems include cyber-physical systems, robot formations, vibration, viscoelasticity, and others (see, for further details [1]–[7]). Thus, developing accurate low order models for large-scale complex systems is important for controlling and designing tasks [8]. In [9]–[11] it is shown that for some network configurations of elements, the equivalent behavior of the system can be represented by implicitly defined integro-differential operators. Fractional order systems are cast as a subset of implicit operators in [11], asserting in this manner that its study could go beyond the use of fractional calculus. In relatively simple cases, the implicit operator describing the system dynamics is the solution to a quadratic operator equation with the implicit operator as the quadratic variable and with known operator coefficients. In such a case, the equation can be solved for multiple operator solutions. However, the operator that is the solution is irrational.

[1]Guel-Cortez is with Universidad Autónoma de San Luis Potosí (UASLP), Facultad de Ingeniería, Dr. Manuel Nava No. 8, San Luis Potosí, S.L.P., México. ajcolorfull@gmail.com.

[2]Bill Goodwine and Mihir Sen are with the Department of Aerospace & Mechanical Engineering, University of Notre Dame, Notre Dame, IN 46556 USA bill@controls.ame.nd.edu and msen@nd.edu.

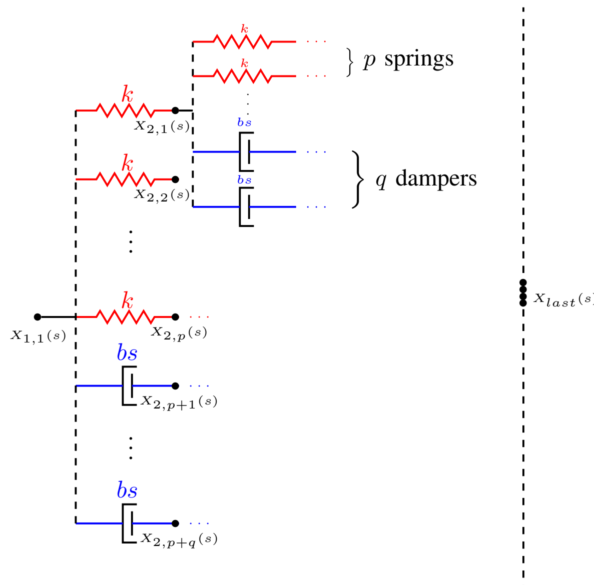


Fig. 1. Networked mechanical system.

We consider the system illustrated in Fig. 1, which is a networked mechanical system with a graph structure of a tree graph. Specifically, at each node in the system, the subsequent generation has $p+q$ nodes where p of the nodes are attached by a spring and q of the nodes are attached by a damper to the previous generation. In the specific case when $p = 1$ and $q = 1$, the system reduces to a well known fractional order system [12]. For the cases where either $p > 1$ or $q > 1$, we have previous results presented in [12], [13] that study its time response but by means of approximations and non-analytical results.

The goal of this research is to develop an analytical way for analyzing the behaviour of complex systems modeled by implicitly defined operators. For such a purpose, this work presents a complex-variable based analysis to obtain the analytical impulse response of the system by means of the Inverse Laplace Transform (ILT) for the irrational transfer function describing the dynamics of the mechanical network with $p$ springs and $q$ dampers. This time domain solution, which is in terms of the parameters will permit us to understand the physics in the phenomenon, ultimately leading to better

978-1-5386-7928-9/$31.00 ©2019 AACC

design and control of such systems.

Throughout the paper the following standard notation is adopted: $\mathbb{C}$ is the set of complex numbers, and $j := \sqrt{-1}$. For $z \in \mathbb{C}$, $\bar{z}$, $\Re(z)$ and $\Im(z)$ define the complex conjugate, the real and the imaginary part of $z$. $\mathrm{Erf}(z)$ is the well known error function of $z$ and $\mathbb{R}$ is the set of real numbers.

## II. BACKGROUND

Consider the network of dampers and springs as illustrated in Figure 1 which has been originally presented as a viscoelastic model from [14] when $p = q = 1$, but can be generally considered as a graph where each node is a mass and each edge is either a spring or a damper (see [13]) or in practical terms as a type of formation robots wherein each robot controls its position relative to its neighbors in accordance with a potential or viscous-like relationship (for further details, see [12]). This network is a tree where each subsequent generation contains $p$ springs and $q$ dampers or more generally speaking $p$ edges with operator $G_1$ and $q$ with operator $G_2$. Let $G_\infty$ be defined as the operator representing the relationship between $x_{1,1}$ and $x_{last}$. In this mechanical network $G_\infty$ stands for the force on the rightmost node as a function of the relative position of $x_{last}$ with respect to $x_{1,1}$ *i.e.*,

$$m_{last} s^2 X_{last}(s) = G_\infty(s) \left( X_{1,1}(s) - X_{last}(s) \right), \quad (1)$$

where $G_\infty(s)$ can be found by using the following.

*Proposition 2.1 (from [13]):* The operator $G_\infty(s)$ satisfying the relation $F(s) = G_\infty(s) \Delta X(s)$ where $\Delta X(s)$ is the Laplace transformed difference of position between the first node $x_{1,1}$ and the last node $x_{last}$ of a network of springs and dampers interconnected as in Figure 1 is given by

$$\begin{aligned} G_\infty(s) &= \tfrac{1}{2} \left[ (p-1)k + (q-1)bs \right] \\ &\pm \tfrac{1}{2} \sqrt{\left[ (p-1)k + (q-1)bs \right]^2 + 4(p+q-1)kbs}, \end{aligned} \quad (2)$$

for $p \geq 1$, $q \geq 1$ and initial conditions for each element in the tree equal to zero.

By using Proposition 2.1, we have that the transfer function that relates the position of the last elements $x_{last}$ with the first one $x_{1,1}$ is

$$G_x(s) = \frac{X_{last}(s)}{X_{1,1}(s)} = \frac{G_\infty(s)}{m_{last} s^2 + G_\infty(s)}. \quad (3)$$

### A. Multivalued functions and the inversion formula

In complex analysis, expression (3) is considered as a multivalued function. Hence, for computing its ILT, we have to consider the location of its Branch Points (BP) and Branch Cuts (BC) in addition to common singularities like poles (see, for further details [15]). To obtain the ILT of any multivalued function, we follow the procedure described in [15] and use the common inversion formula given by

$$f(t) = \frac{1}{j2\pi} \int_{\gamma - j\infty}^{\gamma + j\infty} F(s) e^{st} ds = \frac{1}{j2\pi} \int_{\mathbf{Br}} F(s) e^{st} ds, \quad (4)$$

where **Br** stands for the path $\gamma - j\infty$ to $\gamma + j\infty$ with $\gamma \in \mathbb{R}$ to the right of all singularities of $F(s)$, known as *Bromwich path* considered in the region of convergence (for instance, see [16]). Additionally, it will be useful to have in mind the *Cauchy Residue* Theorem of complex variables (see [15]).

## III. MAIN RESULTS

Taking into consideration the transfer function given by (3), our objective is to solve the following problems.

*Problem 1:* To study the dynamics of the last elements $x_{last}(t)$ in an infinite generation tree-like network of simple mechanical components, as the one shown in Figure 1 by describing a time response of the system in terms of its parameters using the transfer function (3).

*Problem 2:* To compare the infinite network or Infinite Generations System (IGS) response with a Finite Generations System (FGS) to validate how our model can be used instead of a very large system of differential equations.

Consider the general case where we have multiple springs and dampers in (3), then we can write it as follows

$$G_x(s) = \frac{X_{last}(s)}{X_{1,1}(s)} = \frac{G_\infty}{m_{last} s^2 + G_\infty} = \frac{\varrho + \sigma s \pm \sqrt{(\varrho + \sigma s)^2 + \varsigma s}}{m s^2 + \varrho + \sigma s \pm \sqrt{(\varrho + \sigma s)^2 + \varsigma s}}, \quad (5)$$

where $\varrho = (p-1)k$, $\sigma = (q-1)b$, $\varsigma = 4(p+q-1)kb$ and $m = 2m_{last}$.

In the following subsections, we detail the impulse response of system (5) by studying, individually, four possible cases we consider important when constructing the infinite tree of simple mechanical components in order to understand the physical behavior of the system. Due to space limitations we only give proof of the more illustrative cases.

### A. Simple binary tree network with one spring and one damper

When $p = 1$ and $q = 1$ in (5) this gives

$$G_x(s) = \frac{X_{last}(s)}{X_{1,1}(s)} = \frac{G_\infty(s)}{m_{last} s^2 + G_\infty(s)} = \frac{\pm\sqrt{\varsigma s}}{m s^2 \pm \sqrt{\varsigma s}}. \quad (6)$$

*Proposition 3.1:* (*One spring and one damper infinite tree response.*) Given system (6), its impulse response is described by

$$\begin{aligned} x_{last}(t) = &\frac{\sqrt[3]{\varsigma} e^{-\frac{\sqrt[3]{\varsigma} t}{2m^{2/3}}} \left( -e^{\frac{3\sqrt[3]{\varsigma} t}{2m^{2/3}}} + \sqrt{3} \sin\left( \frac{\sqrt{3}\sqrt[3]{\varsigma} t}{2m^{2/3}} \right) + \cos\left( \frac{\sqrt{3}\sqrt[3]{\varsigma} t}{2m^{2/3}} \right) \right)}{3m^{2/3}} \\ &\pm \sum_{\ell=1}^{3} z_\ell \left[ \sqrt{\varsigma} \left( \sqrt{r_\ell} e^{r_\ell t} \, \mathrm{Erf}\left( \sqrt{r_\ell t} \right) + \frac{1}{\sqrt{\pi}\sqrt{t}} \right) \right], \end{aligned} \quad (7)$$

where,

$$
\begin{aligned}
r_1 &= \frac{\sqrt[3]{\varsigma}}{m^{2/3}}, & z_1 &= \frac{m^{7/3}}{\left(1+\sqrt[3]{-1}\right)\left(1+(-1)^{2/3}\right)\sqrt[3]{\varsigma}},\\
r_2 &= -\frac{\sqrt[3]{-1}\,\sqrt[3]{\varsigma}}{m^{2/3}}, & z_2 &= \frac{m^{7/3}}{\left(\sqrt[3]{-1}-1\right)\left(1+\sqrt[3]{-1}\right)\sqrt[3]{\varsigma}}, \qquad (8)\\
r_3 &= \frac{(-1)^{2/3}\,\sqrt[3]{c}}{m^{2/3}}, & z_3 &= \frac{\sqrt[3]{-1}m^{7/3}}{\left(\sqrt[3]{-1}-1\right)\left(1+(-1)^{2/3}\right)\sqrt[3]{\varsigma}}.
\end{aligned}
$$

*Remark 1:* Mathematically $G_\infty(s)$ has two solutions according to (2). However, in the present situation the solution with the plus sign is the one with physical significance and therefore this paper will only consider that case.

### *B. Network with multiple springs and one damper*

Consider now the case $p \geq 1$ and $q = 1$ in (5) such that

$$
G_x(s) = \frac{X_{last}(s)}{X_{1,1}(s)} = \frac{G_\infty(s)}{m_{last}s^2+G_\infty(s)} = \frac{\varrho\pm\sqrt{\varrho^2+\varsigma s}}{ms^2+\varrho\pm\sqrt{\varrho^2+\varsigma s}}. \qquad (9)
$$

*Proposition 3.2: (Network with multiple springs and one damper.)* Given system (9),we can rewrite it as

$$
G_x(s) = H_1(s)+H_2(s) = \frac{\varrho ms-\varsigma}{m^2s^3+2\varrho ms-\varsigma}+\frac{ms\sqrt{\varrho^2+\varsigma s}}{m^2s^3+2\varrho ms-\varsigma}. \qquad (10)
$$

Furthermore, its impulse response when $G_x(s)$ has poles of multiplicity one (none of them inside the BC) is defined by

$$
x_{last}(t) = \sum_{\ell=1}^{3} z_\ell e^{r_\ell t} + \sum_{\ell=1}^{3} w_\ell f_\ell(t). \qquad (11)
$$

If two of the poles of $G_x(s)$ are complex conjugates, then

$$
\begin{aligned}
x_{last}(t) =& z_1 e^{r_1 t} + 2|z_2| e^{\mathbf{J}_2 t}\cos\left(\mathbf{K}_2 t + \arg(z_2)\right)\\
&+\sum_{\ell=1}^{3} w_\ell f_\ell(t), \qquad (12)
\end{aligned}
$$

where $\varrho$, $\varsigma$ and $m$ are defined as previously and $r_\ell$ are the poles of $G_x(s)$ defined as: $r_1 = \mathbf{J}_1$, $r_2 = \mathbf{J}_2 + j\mathbf{K}_2$ and $r_3 = \bar{r}_2$, with $\mathbf{J}_{1,2}, \mathbf{K}_{1,2} \in \mathbb{R}$ and

$$
\begin{aligned}
z_\ell =& \lim_{s\to r_\ell}(s-r_\ell)H_1(s),\\
y_\ell =& \lim_{s\to r_\ell}\frac{(s-r_\ell)}{\sqrt{s+q_p}}H_2(s), \qquad (13)\\
f_\ell(t) =& \sqrt{q_p+r_\ell}\,e^{r_\ell t}\,\mathrm{Erf}\left(\sqrt{t(q_p+r_\ell)}\right)+\frac{e^{-q_p t}}{\sqrt{\pi}\sqrt{t}},
\end{aligned}
$$

with $z_2 = \bar{z}_3$, $y_2 = \bar{y}_3$ and $\ell = 1, 2, 3$. Finally, $q_p = \frac{\varrho^2}{\varsigma}$ which corresponds to the BP of $H_2(s)$.

*Proof:* First, we can see that (10) corresponds to the rationalized version of system (9). By considering the case where the poles of the characteristic polynomial

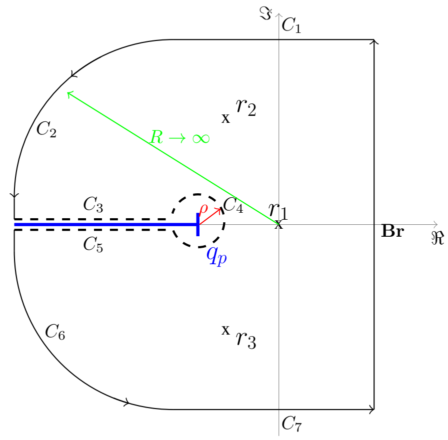


Fig. 2. Integration path of Eq. 16-Proposition 3.2.

$m^2s^3 + 2\varrho ms - \varsigma$ have multiplicity of one, such that its poles are: $r_1, r_2$ and $r_3$, and we have that:

$$
h_1(t) = \mathscr{L}^{-1}\left[H_1(s)\right] = \mathscr{L}^{-1}\left[\frac{\varrho ms-\varsigma}{m^2s^3+2\varrho ms-\varsigma}\right] = \sum_{\ell=1}^{3} z_\ell e^{r_\ell t},
$$

where $\quad z_\ell = \lim_{s\to r_\ell}(s-r_\ell)H_1(s),$

for the first term in (10). Hence, the final result is obtained by solving:

$$
h_2(t) = \mathscr{L}^{-1}\left[H_2(s)\right] = \mathscr{L}^{-1}\left[\frac{ms\sqrt{\varrho^2+\varsigma s}}{m^2s^3+2\varrho ms-\varsigma}\right]. \qquad (14)
$$

By using partial fraction expansion in (14) we have

$$
H_2(s) = \sqrt{s+q_p}\sum_{\ell=1}^{3}\frac{y_\ell}{s-r_\ell}, \qquad (15)
$$

where $y_\ell$ is given by Eq. (13). Each fraction can be inverted by using the integration contour depicted in Fig. 2, while, $r_\ell$ is not inside the BC *i.e.*, $\Re(r_\ell) > \Re(-q_p) \vee \Im(r_\ell) \neq \Im(q_p)$. Then, its ILT can be found by solving the following integral for each $\ell$:

$$
\begin{aligned}
\int_\Gamma \frac{y_\ell\sqrt{s+q_p}}{s-r_\ell}e^{st}ds =& \int_{\mathbf{Br}+C_1+C_2+\cdots+C_7}\frac{y_\ell\sqrt{s+q_p}}{s-r_\ell}e^{st}ds\\
=& 2j\pi\left[\lim_{s\to r_\ell} y_\ell\sqrt{s+q_p}\,e^{st}\right]. \qquad (16)
\end{aligned}
$$

Since $\int_{C_1+C_2+C_4+C_6+C_7} = 0$, we only need to analyze $C_3$ and $C_5$, to obtain

$$
\int_{C_3+C_5} = -2j\int_{q_p}^{\infty}\frac{y_\ell\sqrt{x-q_p}}{x+r_\ell}e^{-xt}dx. \qquad (17)
$$

The integral in the right side of (17) has a solution

$$
\begin{aligned}
\int_{q_p}^{\infty}\frac{y_\ell\sqrt{x-q_p}}{x+r_\ell}e^{-xt}dx =& y_\ell\pi\sqrt{q_p+r_\ell}\,e^{r_\ell t}\mathrm{Erf}\left(\sqrt{t}\sqrt{q_p+r_\ell}\right)\\
&-\pi y_\ell\sqrt{q_p+r_\ell}\,e^{r_\ell t}+y_\ell\frac{\sqrt{\pi}e^{-q_p t}}{\sqrt{t}}.
\end{aligned}
$$

Then from (16)

$$\frac{1}{2\pi j}\int_{\mathbf{Br}} \frac{y_\ell\sqrt{s+q_p}}{s-r_\ell}e^{st}ds = y_\ell f_\ell(t), \tag{18}$$

where $f_\ell(t)$ is defined as in (13). Finally, $x_{last}(t) = h_1(t) + h_2(t)$. ■

### C. Mechanical network with multiple springs and dampers, $p \geq 2$ and $q \geq 2$

*Proposition 3.3 (Branch points locations.):* Given $p \geq 2$ and $q \geq 2$, system $G_x(s)$ defined as (5) only has real Branch Points (BPs) which are distinct and negative.

*Proposition 3.4:* (*Network with multiple springs and dampers $x_{last}(t)$ response.*) Given system (5), we can rewrite it as

$$\begin{aligned} G_x(s) &= H_1(s) + H_2(s) \\ &= \tfrac{ms(\varrho+\sigma s)-\varsigma}{m^2s^3+2ms(\varrho+\sigma s)-\varsigma} + \tfrac{s\sigma\sqrt{s^2+(\frac{2\varrho\sigma+\varsigma}{\sigma^2})s+(\frac{\varrho}{\sigma})^2}}{m(s^3+\frac{2ms(\varrho+\sigma s)}{m^2}-\frac{\varsigma}{m^2})}. \end{aligned} \tag{19}$$

Furthermore, its impulse response for $p \geq 2$ and $q \geq 2$ using the positive solution and considering the case where $G_x(s)$ has poles of multiplicity one with none of them inside the BC of $H_2(s)$ is given by

$$x_{last}(t)=\sum_{\ell=1}^{3} z_\ell e^{r_\ell t}+\sum_{\ell=1}^{3} y_\ell e^{r_\ell t}-\mathbf{M}(t). \tag{20}$$

When $G_x(s)$ has complex poles we have

$$\begin{aligned} x_{last}(t)=&z_1e^{r_1t} + 2|z_2|e^{\mathbf{J}_2t}\cos\left(\mathbf{K}_2t + \arg(z_2)\right) \quad (21)\\ &y_1e^{r_1t} + 2|y_2|e^{\mathbf{J}_2t}\cos\left(\mathbf{K}_2t + \arg(y_2)\right) - \mathbf{M}(t), \end{aligned}$$

for $p \gg 2$ and $q \gg 2$ the solution is approximated by

$$\begin{aligned} x_{last}(t) \approx\ & z_1e^{r_1t} + 2|z_2|e^{\mathbf{J}_2t}\cos\left(\mathbf{K}_2t + \arg(z_2)\right) \\ &+ y_1e^{r_1t} + 2|y_2|e^{\mathbf{J}_2t}\cos\left(\mathbf{K}_2t + \arg(y_2)\right), \end{aligned} \tag{22}$$

where $\varrho$, $\sigma$, $\varsigma$ and $m$ are defined as previously and $r_\ell$ are the poles of $G_x(s)$ defined as $r_1 = \mathbf{J}_1$, $r_2 = \mathbf{J}_2 + j\mathbf{K}_2$, and $r_3 = \bar{r}_2$, with $\mathbf{J}_{1,2}, \mathbf{K}_{1,2} \in \mathbb{R}$. Besides:

$$\begin{aligned} z_\ell &= \lim_{s\to r_\ell}(s-r_\ell)H_1(s), \quad y_\ell = \lim_{s\to r_\ell}(s-r_\ell)H_2(s), \\ \mathbf{M}(t) &= \frac{1}{\pi}\int_0^{v_2-v_1}\tfrac{\sigma(v_2-x)\sqrt{x(v_2-v_1-x)}}{mP(x)}e^{(v_2-x)t}dx, \\ P(x) &= \tfrac{2(v_2-x)(\varrho+\sigma(v_2-x))}{m} - \tfrac{\sigma}{m^2} + (v_2-x)^3. \end{aligned} \tag{23}$$

with $\ell = 1, 2, 3$.

*Proof:* $G_x(s)$ in (5) can be rationalized by multiplying and dividing by $ms^2+\varrho+\sigma s\mp\sqrt{(\varrho+\sigma s)^2+\varsigma s}$ this gives expression (19) as stated. The ILT of $H_1(s)$, which can be computed easily, and therefore we will focus on the ILT of $H_2(s)$.

$H_2(s)$ is a multivalued function with 3 poles and 2 BPs. According to Proposition 3.3, we can conclude that

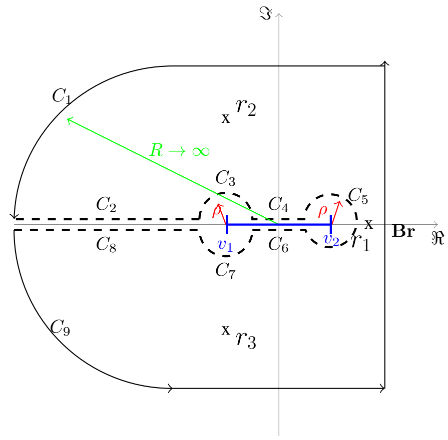


Fig. 3. Integration contour of Eq. (24)-Proposition 3.4, $r_1$ is considered to be inside $\Gamma$.

there exist three possible integration contours we have to consider in order to find the ILT of $H_2(s)$. Here we will consider only one of them, where the real root $r_1$ of the characteristic equation is inside the contour $\Gamma = \mathbf{Br} + C_1 + C_2 + \cdots + C_9$ as depicted in Figure 3. The other cases would be: $r_1$ is inside the BC from $v_1$ to $v_2$ and $r_1$ would be somewhere between $\infty$ and $v_1$. Then, to obtain $\mathscr{L}^{-1}$ we have to solve the following integral:

$$\begin{aligned} \int_\Gamma H_2(s)e^{st}ds=&\int_{Br+C_1+C_2+\cdots+C_9} H_2(s)e^{st}ds \\ &=2j\pi\left[\sum_{\ell=1}^{3}\lim_{s\to r_\ell}(s-r_\ell)H_2(s)e^{st}\right]. \end{aligned} \tag{24}$$

We can see that $\int_{\Gamma_0} = 0$, for $\Gamma_0 = C_1+C_2+C_3+C_5+C_7+C_8+C_9$. In order to do the integration along $C_4$ and $C_6$ , let us do the parameterization $s = xe^{\pm j\pi} \pm j\delta + v_2$ where positive and negative signs correspond to $C_4$ and $C_6$, respectively, $x \in (0, v_2-v_1)$ and $\delta$ is a small positive number which tends to zero. Some algebra yields

$$\begin{aligned} \int_{C_4+C_6} & \tfrac{s\sigma\sqrt{(s-v_1)(s-v_2)}}{m(s^3+\frac{2ms(\varrho+\sigma s)}{m^2}-\frac{\varsigma}{m^2})}e^{st}ds = \\ &= \int_0^{v_2-v_1} 2j\tfrac{\sigma(v_2-x)\sqrt{x(v_2-v_1-x)}}{mP(x)}e^{(v_2-x)t}dx, \end{aligned}$$

where $P(x)$ is defined as in (23). Analyzing the last integral we can see that $|P(x)| > |\sigma(v_2-x)\sqrt{x(v_2-v_1-x)}|$ and if we add more elements $|P(x)|$ starts to increase making this integral to have a very small value. Hence, we can say this value is negligible for describing the whole behaviour of $x_{last}(t)$ when $p \gg 2$ and $q \gg 2$. ■

### D. Mechanical network with one spring and multiple dampers, $p = 1$ and $q \geq 2$

*Proposition 3.5 (Multiple dampers one spring case.):* Consider the system described as in (5) and $H_1(s)$ and

$H_2(s)$ as in Proposition 3.4, for $p = 1$ and $q \geq 2$, the impulse response of the system is given by

$$x_{last}(t) = \sum_{\ell=1}^{3} z_\ell e^{r_\ell t} + \sum_{\ell=1}^{3} y_\ell e^{r_\ell t} - \mathbf{N}(t). \quad (25)$$

When $r_2$ and $r_3$ are complex conjugated we have

$$x_{last}(t) = z_1 e^{r_1 t} + 2|z_2| e^{\mathbf{J}_2 t} \cos(\mathbf{K}_2 t + \arg(z_2)) \quad (26)$$
$$y_1 e^{r_1 t} + 2|y_2| e^{\mathbf{J}_2 t} \cos(\mathbf{K}_2 t + \arg(y_2)) - \mathbf{N}(t),$$

where $\varrho$, $\sigma$, $\varsigma$ and $m$ are defined as previously and $r_\ell$ are the poles of $G_x(s)$ defined as $r_1 = \mathbf{J}_1$, $r_2 = \mathbf{J}_2 + j\mathbf{K}_2$, and $r_3 = \bar{r}_2$, with $\mathbf{J}_{1,2}, \mathbf{K}_{1,2} \in \mathbb{R}$. Besides:

$$z_\ell = \lim_{s \to r_\ell} (s - r_\ell) H_1(s), \quad y_\ell = \lim_{s \to r_\ell} (s - r_\ell) H_2(s),$$
$$\mathbf{N}(t) \frac{1}{\pi} \int_0^{q_p} \frac{m\sigma x \sqrt{x(q_p - x)}}{m^2 x^3 - 2m\sigma x^2 + \varsigma} e^{-xt} dx, \quad q_p = \frac{\varsigma}{\sigma^2}, \quad (27)$$

with $\ell = 1, 2, 3$.

## IV. TIME DOMAIN VALIDATION SIMULATIONS

As stated in Problem 2, we aim to prove the efficiency of our results when trying to model tree-networks of finite generations. This could be useful for the avoiding of long computations due to the high number of differential equations needed when adding large levels to the tree. In the next figures we show some simulations which compare our analytical expressions with the time response of a FGS. The FGS solution $x_{last_j}(t)\ \forall\ j = 1, 2, \cdots, N$, is computed in Octave by using *lsode()* routine. It is worth mentioning that in the FGS every node in the last generation is considered to have the same position.

For computing our FGS responses, we have taken an impulse-like input to be defined as: $x_{1,1}(t) = \delta_\alpha(t - 1) \approx \frac{1}{|\alpha|\sqrt{\pi}} e^{-\left(\frac{t-1}{\alpha}\right)^2}$. Such an input is time shifted one time unit in order to obtain better numerical results when solving the differential equations of the FGSs. The system parameters are taken as $b = \frac{1}{10}$ and $k = 2$. Every $x_{last}(t)$ expressed analytically from Propositions 3.1 to 3.5 was also time shifted by 1 time unit, in order to make the comparison of the impulse responses. Furthermore, we add bar plots with error-index values. The error measured used is the common integral square error (ISE), defined here as: $\mathbf{E}_I = \int_0^{30} \epsilon(t)^2 dt$, where $\epsilon(t) = x_{last}(t-1)H(t-1) - x_{last_j}(t)$, $H(t)$ stands for the Heaviside step function. The expression $i$ FGS in the captions of Figs. 4 to 7 for $i = 1, 2, 3, \ldots$ stands for the exact number of finite generations used when computing the time domain solution in Octave.

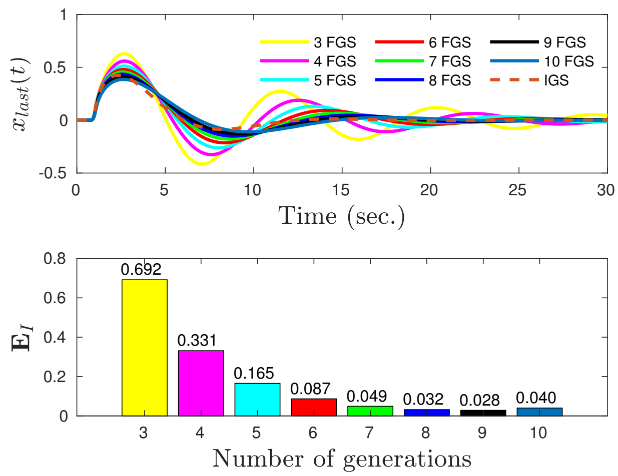


Fig. 4. Impulse response comparison for the case $p = 1$ and $q = 1$. Here, $x_{last}$ is used as in Proposition 3.1 but time-shifted 1 time unit and $x_{1,1} = \delta_{\frac{1}{8}}(t - 1)$.

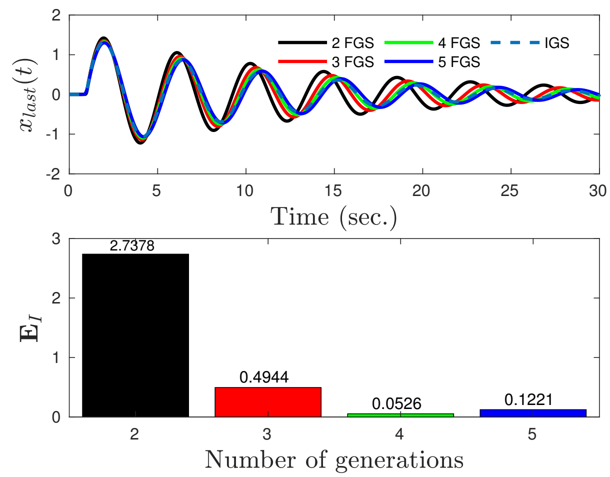


Fig. 5. Impulse response comparison for the case $p = 2$ and $q = 1$. Here, $x_{last}$ is used as in Proposition 3.2 but time-shifted 1 time unit and $x_{1,1} = \delta_{\frac{1}{15}}(t - 1)$.

## V. CONCLUSIONS AND FUTURE WORK

This paper illustrates a means for determining the time response of an infinite tree of springs and dampers whose dynamics are given by an implicitly-defined operator. We have shown how the infinite order model can be used as a model for FGSs by comparing impulse responses. The results of the comparisons show a slight difference in terms of amplitude but sometimes large difference in time phase which increases the ISE. The computation time increases exponentially when adding more generations, which makes it difficult to have quick and accurate numerical results for more generations in each of the cases presented. In Fig. 4 we see how the

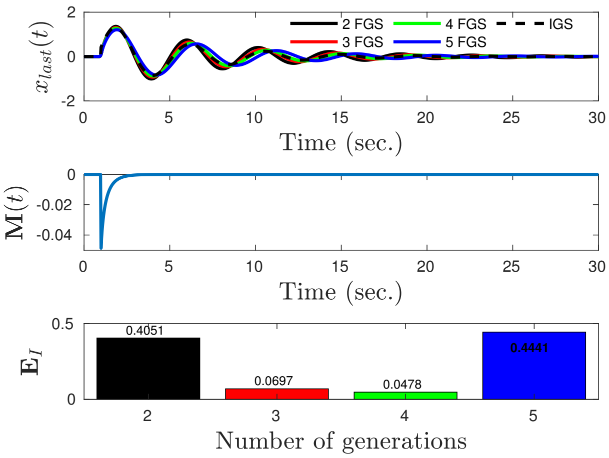


Fig. 6. Impulse response comparison for the case $p = 2$ and $q = 2$. Here, $x_{last}$ is used as in Proposition 3.4 but time-shifted 1 time unit and $x_{1,1} = \delta_{\frac{1}{15}}(t-1)$. The term $\mathbf{M}(t)$ is plotted to show how fast it goes to zero, so that, this term can be avoided when using expression (20).

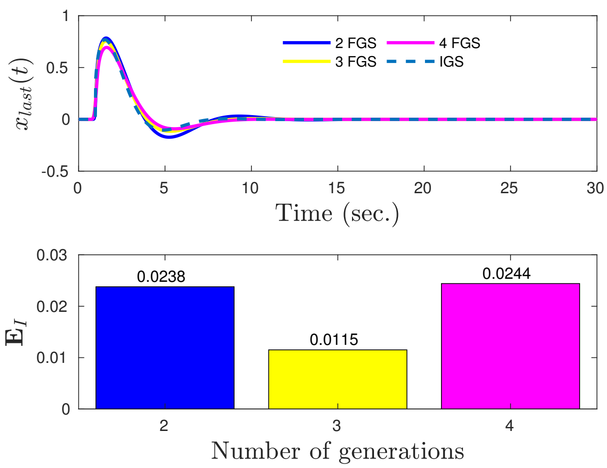


Fig. 7. Impulse response comparison for the case $p = 1$ and $q = 5$. Here, $x_{last}$ is used as in Proposition 3.5 but time-shifted 1 time unit and $x_{1,1} = \delta_{\frac{1}{15}}(t-1)$.

ISE decreases exponentially but once we get to the 10th generation response the error slightly increases, perhaps due to numerical error. The difference in the number of finite generations computed in each of the Figs. 4 to 7 corresponds to an increase in the computational effort of finding the time domain response which did not allow us to compute the same number of generations for each case. Therefore, future efforts will be focused on proving convergence of the infinite generation irrational system to the proposed large, but finite model by other means such as using a phase-magnitude error analysis of the responses and a general frequency response analysis. These results could be easier to achieve thanks to the time domain responses presented in this work. Finally, our closed form time responses naturally lead to other possible future analysis useful in systems and control for systems described by implicit operators such as stability, design, or system identification.

## ACKNOWLEDGMENT

The work of A.-J. Guel-Cortez has been supported by CONACyT-México and partially supported by Secretaría de Investigación y Posgrado-UASLP-México.

## REFERENCES

[1] B. Goodwine, “Modeling a multi-robot system with fractional-order differential equations,” in *Proceedings of the IEEE International Conference on Robotics and Automation*, pp. 1763–1768, 2014.

[2] P. Derler, E. A. Lee, and A. S. Vincentelli, “Modeling cyber-physical systems,” *Proceedings of the IEEE*, vol. 100, no. 1, pp. 13–28, 2012.

[3] M. Roemer and G. Kacprzynski, “Advance diagnostics and prognostics for gas turbine engine risk assessment,” in *Aerospace Conference Proceedings*, vol. 6, pp. 345–353, IEEE, 2000.

[4] M. H. Mehrabi, M. Suhatril, Z. Ibrahim, S. S. Ghodsi, and H. Khatibi, “Modeling of a viscoelastic damper and its application in structural control,” *PLOS ONE*, vol. 12, pp. 1–22, 06 2017.

[5] T. D. Popescu, D. Aiordachioaie, and M. Manolescu, “Change detection in vibration analysis  a review of problems and solutions,” in *2017 5th International Symposium on Electrical and Electronics Engineering (ISEEE)*, 2017.

[6] J. F. Kelly and R. J. MacGough, “Fractal ladder models and power law wave equations,” *Journal of the acoustical society of america*, vol. 126, no. 4, pp. 2072–2081, 2009.

[7] C. M. Ionescu, J. A. T. Machado, and R. De Keyser, “Modeling of the lung impedance using a fractional-order ladder network with constant phase elements,” *IEEE Transactions on Biomedical Circuits and Systems*, vol. 5, pp. 83–89, Feb 2011.

[8] A.-J. Guel-Cortez, M. Sen, C.-F. Méndez-Barrios, and B. Goodwine, “Fractional-*pd*$^{\mu}$ controllers for implicitly defined systems,” in *International conference on control, decision and information technologies*, (Paris, France), April 23-26 2019, to be published.

[9] K. Leyden, M. Sen, and B. Goodwine, “Models from an implicit operator describing a large mass-spring-damper network,” *9th Vienna International Conference on Mathematical Modelling*, vol. 51, no. 2, pp. 831–836, 2018.

[10] J. Mayes and M. Sen, “Approximation of potential-driven flow dynamics in large-scale self-similar tree networks,” *Proceedings of the Royal Society of London A: Mathematical, Physical and Engineering Sciences*, vol. 467, no. 2134, pp. 2810–2824, 2011.

[11] M. Sen, J. P. Hollkamp, F. Semperlotti, and B. Goodwine, “Implicit and fractional-derivative operators in infinite networks of integer-order components,” *Chaos, Solitons & Fractals*, vol. 114, pp. 186–192, 2018.

[12] B. Goodwine, “Fractional-order approximations to implicitly-defined operators for modeling and control of networked mechanical systems,” in *2016 IEEE International Symposium on Intelligent Control (ISIC)*, pp. 1–7, 2016.

[13] B. Goodwine, “Approximations for implicitly-defined dynamics of networks of simple mechanical components,” in *2018 26th Mediterranean Conference on Control and Automation (MED)*, pp. 454–459, 2018.

[14] N. Heymans and J. C. Bauwens, “Fractal rheological models and fractional differential equations for viscoelastic behavior,” *Rheologica Acta*, vol. 33, pp. 210–219, May 1994.

[15] H. Cohen, *Complex analysis with applications in science and engineering*. Springer, 2007.

[16] W. T. Thomson, *Laplace Transformation*. New York Prentice-Hall, Inc., 1950.